

## Photoluminescence due to positively charged excitons in undoped GaAs/Al<sub>x</sub>Ga<sub>1-x</sub>As quantum wells

J. L. Osborne,\* A. J. Shields, and M. Pepper\*

*Toshiba Cambridge Research Centre, 260, Science Park, Milton Road, Cambridge CB4 4WE, United Kingdom*

F. M. Bolton and D. A. Ritchie

*Cavendish Laboratory, University of Cambridge, Madingley Road, Cambridge CB3 0HE, United Kingdom*

(Received 31 October 1995; revised manuscript received 17 January 1996)

We study the photoluminescence (PL) spectra of nominally undoped GaAs/Al<sub>0.33</sub>Ga<sub>0.67</sub>As quantum wells, as a function of well width, temperature, excitation energy, and intensity, and an applied magnetic field. A doublet is observed for temperatures below 10 K, whose components we demonstrate derive from the neutral ( $X$ ) and positively charged ( $X^+$ ) excitons. The latter appears due to the binding of excitons to holes in the quantum well originating from the background concentration of acceptors in the Al<sub>0.33</sub>Ga<sub>0.67</sub>As barriers. Our assignment of  $X^+$  is motivated by the striking similarity of the PL spectra to those recorded on quantum wells with acceptors deliberately incorporated in the barriers. Consistent with our assignment, we see a strengthening of the  $X^+$  transition when more holes are introduced into the well by photoexcitation. The dependence of the doublet splitting on well width is in close agreement with a Monte Carlo calculation of the second hole binding energy in  $X^+$ . The PL peak due to  $X^+$  may have been falsely ascribed in previous work to a biexciton. [S0163-1829(96)05519-1]

### I. INTRODUCTION

Low-temperature photoluminescence (PL) spectra of nominally undoped bulk GaAs typically show a number of peaks due to recombination of excitons bound to impurities or defects, with usually only a weak feature arising from the free exciton.<sup>1</sup> In fact, the free exciton has no radiative decay path that conserves both the  $k$  vector and energy.<sup>2</sup> The relative strength of the bound exciton PL derives from the relaxation of the  $k$ -vector conservation rule. Translational invariance is also destroyed in a two-dimensional system, resulting in those excitons lying below the crossing with the light line being able to decay radiatively.<sup>3</sup> Consequently, the PL spectra of GaAs/Al<sub>x</sub>Ga<sub>1-x</sub>As quantum wells are typically dominated by free-exciton recombination. Donor bound excitons, similar to those seen in bulk GaAs, have been reported for wide undoped GaAs/Al<sub>x</sub>Ga<sub>1-x</sub>As quantum wells.<sup>4</sup> However, their observation is rarer in narrower undoped quantum wells, possibly because of the smearing caused by the dependence of the binding energy on the donor position along the growth axis. On the other hand, PL studies of doped GaAs/Al<sub>x</sub>Ga<sub>1-x</sub>As quantum wells have revealed peaks ascribed to donor<sup>5</sup> and acceptor<sup>6</sup> bound excitons.

PL lines below the band-edge free-exciton peak in undoped GaAs/Al<sub>x</sub>Ga<sub>1-x</sub>As quantum wells have also been ascribed to biexcitons, otherwise known as the excitonic molecule, formed when two excitons bind together.<sup>7-10</sup> The splitting of the biexciton line from the free exciton implies a binding energy of about 1 meV. The assignment of the biexciton line by these authors was based largely on its superlinear dependence on the laser excitation intensity. However, Charbonneau *et al.*<sup>10</sup> demonstrated that conflicting excitation intensity dependences could be obtained and suggested that donor bound excitons and biexcitons could dominate in wells

grown with and without growth interruptions, respectively.

Recently there has been research into another type of bound<sup>11</sup> exciton: the so-called charged exciton formed when an exciton binds to an electron or hole. Negatively charged excitons ( $X^-$ ) were observed by Kheng *et al.* in CdTe/Cd<sub>x</sub>Zn<sub>1-x</sub>Te quantum wells containing excess electrons due to the barriers being doped with donors.<sup>12</sup> These authors have also reported negatively charged excitons in undoped CdTe/Cd<sub>x</sub>Zn<sub>1-x</sub>Te quantum wells, due to the presence of photoexcited electrons in the well.<sup>13</sup> PL measurements performed on remotely  $n$ -type-doped GaAs/Al<sub>x</sub>Ga<sub>1-x</sub>As quantum wells with a depleting gate contact display a doublet structure at the lowest electron densities.<sup>14-17</sup> The higher and lower components of this doublet have been ascribed to the band-edge neutral ( $X$ ) and negatively charged ( $X^-$ ) excitons, respectively. We observed a strong  $X^-$  transition at excess electron densities of around  $(2-4) \times 10^{10} \text{ cm}^{-2}$  in samples where the effect of the fluctuations in the conduction-band edge due to the donor ions in the barrier was relatively small.<sup>15</sup> On the other hand, Finkelstein *et al.* found that  $X^-$  could persist to higher electron densities in samples with strong inhomogeneities, due to higher doping concentrations and narrower spacer layer thickness between the dopants and well.<sup>16</sup> We have also observed positively charged excitons ( $X^+$ ) in GaAs/Al<sub>x</sub>Ga<sub>1-x</sub>As quantum wells containing excess holes due to remote doping of the barriers with acceptors.<sup>18</sup> At the lowest hole densities the PL spectrum again showed a doublet structure, unambiguously ascribed to recombination involving  $X$  and  $X^+$ .

In this paper we present measurements on nominally undoped GaAs/Al<sub>0.33</sub>Ga<sub>0.67</sub>As quantum wells. Their PL spectra show a doublet structure that is rather similar to that previously observed<sup>14-18</sup> for remotely doped quantum wells at low carrier densities. This leads us to suspect that the lower-

energy component of the doublet seen for the undoped wells may also be due to a charged exciton. We demonstrate that the unavoidable background acceptor concentration in the  $\text{Al}_{0.33}\text{Ga}_{0.67}\text{As}$  barriers is indeed sufficient to produce a significant population of holes, and hence  $X^+$ , in the quantum wells. This conclusion should not be surprising, in view of the fact that  $\text{Al}_x\text{Ga}_{1-x}\text{As}$  grown by molecular-beam-epitaxy (MBE) incorporates a much higher density of impurities than GaAs (Ref. 19) and therefore provides a natural explanation for the extrinsic recombination. Despite the presence of the barrier impurities, we point out that the samples studied here are high quality, as exemplified by excitonic linewidths as narrow as 0.15 meV [full width half maximum (FWHM)].

After a description of our experimental methods, we present PL spectra recorded on several wells of different width as a function of sample temperature, excitation intensity at different laser energies, and applied magnetic field. This systematic study elucidates the origin of the lower-energy peak in the observed PL doublet as due to  $X^+$ , as we discuss in Sec. IV. In Sec. V we discuss the possibility that a very similar PL doublet structure observed previously by other authors in samples similar to our own, which they ascribed to biexciton formation, may actually derive from  $X^+$ .

## II. EXPERIMENTAL METHODS

Four wafers with an identical layer structure were investigated, each consisting of four GaAs quantum wells separated by  $\text{Al}_{0.33}\text{Ga}_{0.67}\text{As}$  barriers grown by MBE on a (100)-oriented, undoped GaAs substrate. The full layer structure consisted of a 1- $\mu\text{m}$  GaAs buffer layer, 300- $\text{\AA}$   $\text{Al}_{0.33}\text{Ga}_{0.67}\text{As}$ , 300- $\text{\AA}$  GaAs quantum well, 300- $\text{\AA}$   $\text{Al}_{0.33}\text{Ga}_{0.67}\text{As}$ , 200- $\text{\AA}$  GaAs, 300- $\text{\AA}$   $\text{Al}_{0.33}\text{Ga}_{0.67}\text{As}$ , 165- $\text{\AA}$  GaAs, 300- $\text{\AA}$   $\text{Al}_{0.33}\text{Ga}_{0.67}\text{As}$ , 140- $\text{\AA}$  GaAs, 3000- $\text{\AA}$   $\text{Al}_{0.33}\text{Ga}_{0.67}\text{As}$ , and 100- $\text{\AA}$  GaAs capping layer. The four samples were nominally identical except for the substrate temperature during growth, which was 630  $^\circ\text{C}$  for sample 1, 650  $^\circ\text{C}$  for sample 2, 630  $^\circ\text{C}$  for sample 3, and 610  $^\circ\text{C}$  for sample 4. Sample 1 was grown two months prior to samples 2–4, at a time when the growth chamber had a higher background impurity concentration.

An indication of the background impurity level is given by the mobilities of ungated high electron mobility transistors (HEMT's) grown in the same MBE chamber. A short time before sample 1, a GaAs/ $\text{Al}_{0.33}\text{Ga}_{0.67}\text{As}$  HEMT with a 200- $\text{\AA}$  spacer layer was grown with a 4-K mobility of  $1.0 \times 10^6 \text{ cm}^2 \text{ V}^{-1} \text{ s}^{-1}$  after illumination. On the other hand, an identical HEMT structure grown around the time of samples 2–4 showed a higher mobility of  $1.8 \times 10^6 \text{ cm}^2 \text{ V}^{-1} \text{ s}^{-1}$  under identical measurement conditions, suggesting that their background impurity concentration was significantly lower. The HEMT mobility generally improves over the several month growth run duration due to the reduction in the level of background impurity concentration in the MBE chamber.

Although none of the layers in the structure were intentionally doped, MBE-grown  $\text{Al}_{0.33}\text{Ga}_{0.67}\text{As}$  is susceptible to the incorporation of significant levels of  $p$ -type dopants, with carbon generally thought to be the principle acceptor species.<sup>19</sup> Daniels *et al.* have studied the background impu-

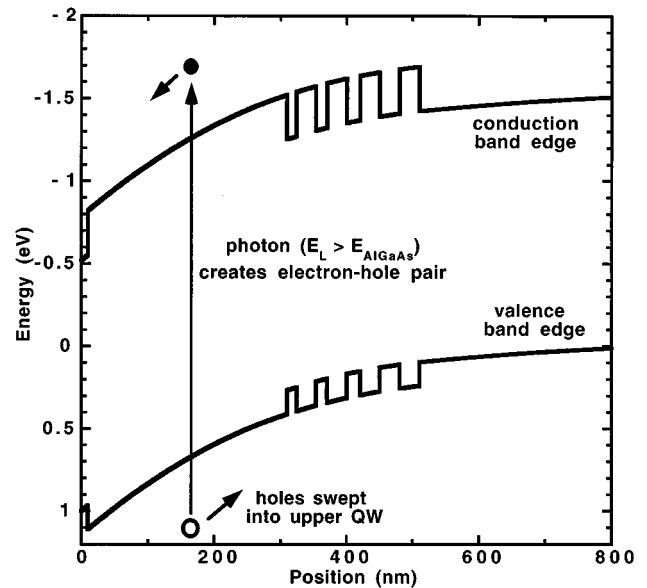


FIG. 1. Conduction- and valence-band profiles across the layer structure. The zero of the position axis corresponds to the front surface of the sample. Electron-hole pairs photoexcited in the front  $\text{Al}_{0.33}\text{Ga}_{0.67}\text{As}$  are separated by the internal field with the holes being swept in the upper 140- $\text{\AA}$  quantum well.

urity densities of  $\text{Al}_x\text{Ga}_{1-x}\text{As}$  layers grown in our MBE machine and found acceptor concentrations of about  $5 \times 10^{15} \text{ cm}^{-3}$ .<sup>20</sup> GaAs grown in the same manner incorporates at least an order of magnitude fewer impurities.

The conduction- and valence-band profiles for the structure studied here are shown in Fig. 1, calculated using the nominal layer widths and a  $p$ -type doping level in the  $\text{Al}_{0.33}\text{Ga}_{0.67}\text{As}$  layers of  $5 \times 10^{15} \text{ cm}^{-2}$ . This acceptor charge produces the curvature of the band edges in the thick front  $\text{Al}_{0.33}\text{Ga}_{0.67}\text{As}$  region. The calculated profiles assume the Fermi level is pinned just above the valence-band edge and midgap by the surface states at the air-semiconductor interface.

The PL spectra were obtained by placing the samples in a variable temperature He cryostat within a split coil superconducting magnet that could apply a field of up to 8 T. The sample was excited with either the 488-nm line of an Ar-ion laser or a tunable Ti:sapphire laser propagating normal to the sample surface. The PL emitted normal to the sample surface was collected and dispersed by a single grating spectrometer of 0.64 m focal length and detected by a liquid-nitrogen-cooled charge coupled device. The incident and the emitted light were circularly polarized with respect to the magnetic-field axis.

## III. PHOTOLUMINESCENCE SPECTRA

Figure 2 plots PL spectra measured for each of the four samples under identical conditions. The excitation energy ( $E_L$ ) and intensity density ( $P_L$ ) were 1.72 eV and 42  $\text{mW cm}^{-2}$ , respectively, while the sample temperature was 2.0 K. Each quantum well shows a strong peak due to the recombination of the free  $1s$  exciton formed between an

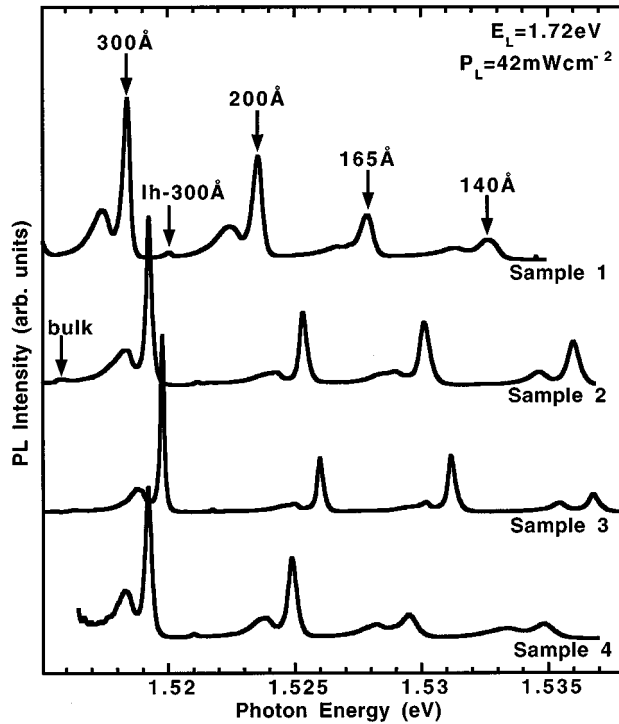


FIG. 2. Comparison of PL spectra obtained from each of the four samples tested.

electron and a heavy hole in their lowest confined subbands,  $e1 - hh1$ , as marked by the arrows for each quantum well of sample 1 in Fig. 2. Notice that each quantum well also displays a weaker PL peak around 0.97–1.35 meV below the free exciton. This feature, which we show later to be due to recombination of an exciton bound to a hole in the quantum well, is the focus of this paper. Notice that the splitting of the two PL peaks of the doublet emanating from each quantum well increases with decreasing well width, as can be seen in Table I.

The three wafers grown around the same time (i.e., samples 2, 3, and 4) show very similar spectra. The differences in the excitonic energies in Fig. 2 suggests a variation in the growth rate between samples. A high degree of layer homogeneity is indicated by the narrow PL linewidths displayed by each sample, which for the 300-Å quantum well is 0.15 meV (FWHM) for samples 2 and 3 and 0.2 meV (FWHM) for sample 4. Sample 1, which was grown two months earlier, shows more significant differences to the others. The PL lines of sample 1 are slightly broader than those of samples 2–4 ( $\approx 0.3$  meV FWHM for the free exciton line of the 300-Å quantum well), which may be due to the higher

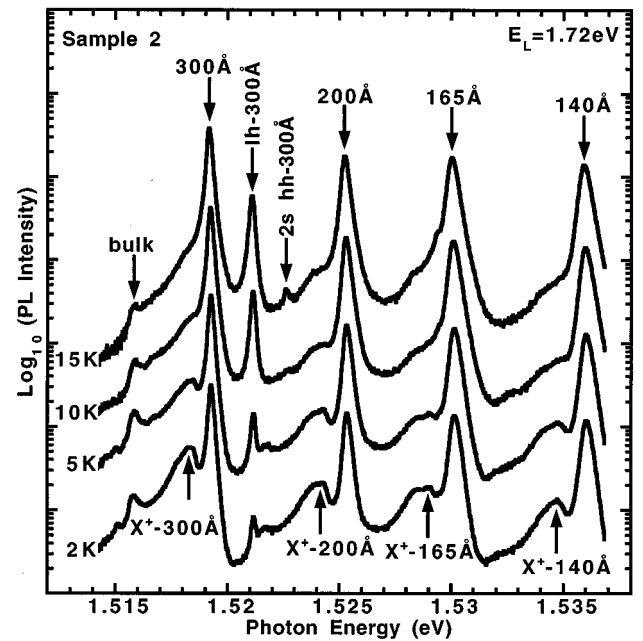


FIG. 3. PL spectra (plotted on a logarithmic scale) recorded on sample 2 at different temperatures.

background impurity concentration at the time sample 1 was grown. Notice too that the lower-energy component of the doublet is stronger relative to its higher-energy companion for each of the wells in sample 1, which we will later also explain by its higher  $\text{Al}_{0.33}\text{Ga}_{0.67}\text{As}$  impurity concentration.

Figure 3 plots PL recorded on sample 2 for different sample temperatures. Notice that at 2 K the lower-energy component of each of the doublets is relatively strong. However, as the temperature is increased the lower-energy peaks weaken sharply, while the higher-energy components strengthen slightly, so that only the latter is readily discernible at 15 K. There is also a strengthening with temperature of the light-hole exciton line of the 300-Å quantum well, in addition to the 2s state of the heavy-hole exciton. A very similar temperature dependence was observed for the PL doublets of the other samples. This behavior demonstrates that the populations of the excitons responsible for the two transitions are in thermal equilibrium. The disappearance of the lower-energy peak with increasing temperature suggests that it arises from a bound exciton, while its higher-energy companion is due to a free exciton. The exciton will dissociate from its binding center at temperatures where the thermal energy exceeds its binding energy. A binding energy of 1 meV, equal to the doublet splitting for the 300-Å quantum well, implies a dissociation temperature of 12 K, in

TABLE I. Splitting of the PL doublet measured for each of the quantum wells in each of the four samples.

Well width (Å)	Binding energy (meV)				
	Sample 1	Sample 2	Sample 3	Sample 4	Average
140	1.35	1.37	1.36	1.33	$1.35 \pm 0.01$
165	1.12	1.12	1.11	1.12	$1.12 \pm 0.01$
200	1.10	1.06	1.10	1.06	$1.08 \pm 0.02$
300	0.98	0.95	0.97	0.96	$0.97 \pm 0.01$

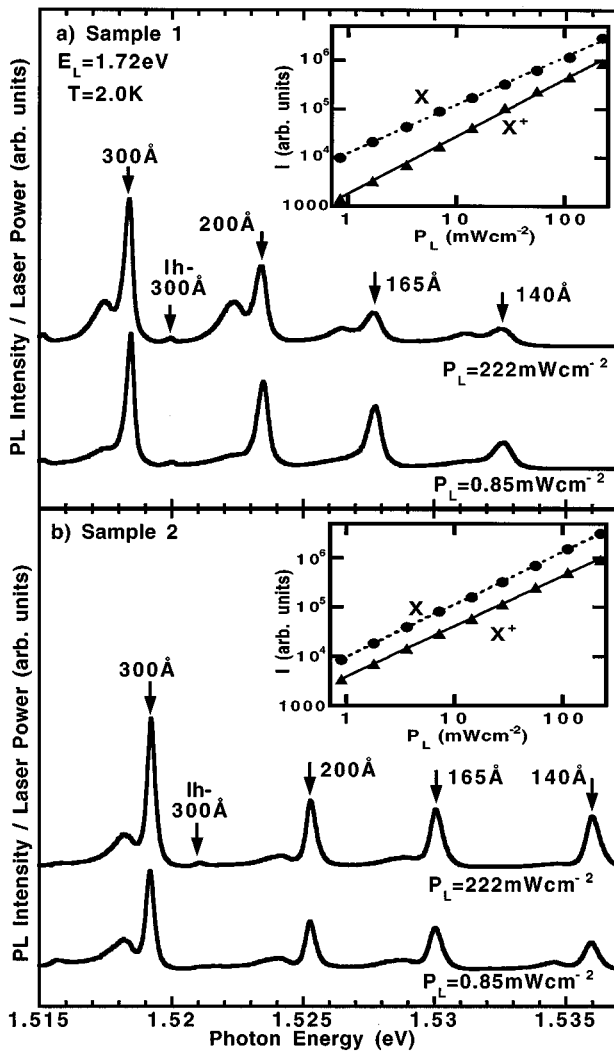


FIG. 4. PL spectra recorded on samples (a) 1 and (b) 2, using relatively strong and weak illumination intensities, for a laser energy smaller than the band gap of the barrier material. The PL intensity is normalized to the illumination intensity. Inset: log-log plot of the unnormalized PL intensity of the two peaks observed for the 300-Å quantum well vs laser intensity (points). The straight lines are fits of the form  $I = A(P_L)^\alpha$ .

good agreement with the dependence shown in Fig. 3.

We measured photoluminescence excitation (PLE) spectra by detecting on the lower-energy peak of the doublet. For each of the quantum wells this showed a strong sharp peak at the energy of the upper energy component of the PL doublet, consistent with it deriving from the free heavy-hole exciton. There was no discernible Stokes shift between the PL and PLE peaks. The PLE spectra also showed a peak to higher energy for each well due to the free light-hole exciton.

We studied the dependence of the PL spectra on the laser excitation density ( $P_L$ ). Figures 4(a) and 4(b) plot the PL spectra recorded from samples 1 and 2, respectively, with a relatively strong and weak excitation intensity. The laser energy was  $E_L = 1.72$  eV for these measurements, which is much less than the band gap of the  $\text{Al}_{0.33}\text{Ga}_{0.67}\text{As}$  barriers ( $E_{\text{Al}_x\text{Ga}_{1-x}\text{As}}$ ). The free exciton from each of the wells is indicated by an arrow in the figure. Since the vertical axis in

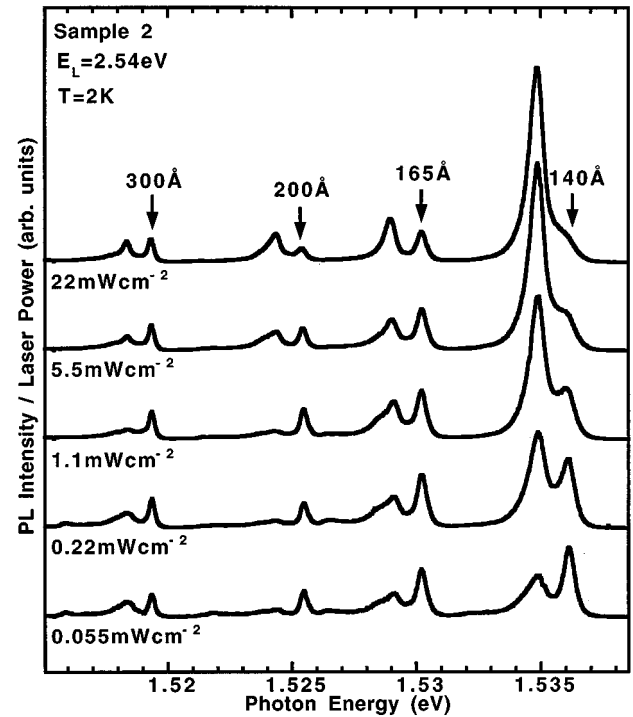


FIG. 5. PL spectra recorded on sample 2 with different excitation intensities for a laser energy larger than the barrier band gap.

Fig. 4 has been normalized to the laser power, it is immediately apparent that the PL intensity is roughly proportional to  $P_L$ . However, a more detailed inspection reveals that the bound exciton PL (lower-energy component of doublet) is stronger relative to the free exciton at higher excitation intensities for sample 1, while, in contrast, it is less prominent at higher power for sample 2.

When the sample is excited with a laser energy above the band gap of the  $\text{Al}_{0.33}\text{Ga}_{0.67}\text{As}$  barriers ( $E_L = 2.54$  eV) a much stronger dependence on the laser power is observed. Since all four samples exhibited a similar dependence on  $P_L$  (for excitation above the barrier), we plot in Fig. 5 representative data taken from sample 2. Notice that at the weakest excitation intensity in Fig. 5, the PL spectrum is similar to those measured for excitation below the barrier band gap, with the free-exciton recombination (marked by the arrows) from each of the wells being stronger than that of the bound exciton. The doublet splitting is the same for photoexcitation above and below the barrier band gap. However, as the laser intensity is increased there is a dramatic strengthening of the bound exciton peak relative to the free exciton of the 140-Å quantum well. Thus, at the highest excitation densities plotted in Fig. 5 the bound exciton PL from the 140-Å quantum well dominates the spectrum. The bound exciton peaks of the other quantum wells also strengthen relative to those of the free exciton, although the dependence is much less dramatic than for the 140-Å well.

Another intriguing phenomenon displayed by sample 1 is the dependence of the PL spectrum on the position of the laser spot on the sample surface. Figure 6 shows PL spectra taken with the spot focused on different regions of the sample separated by approximately  $400 \mu\text{m}$ . The variation in the spectra is particularly pronounced for the 200-Å well. It

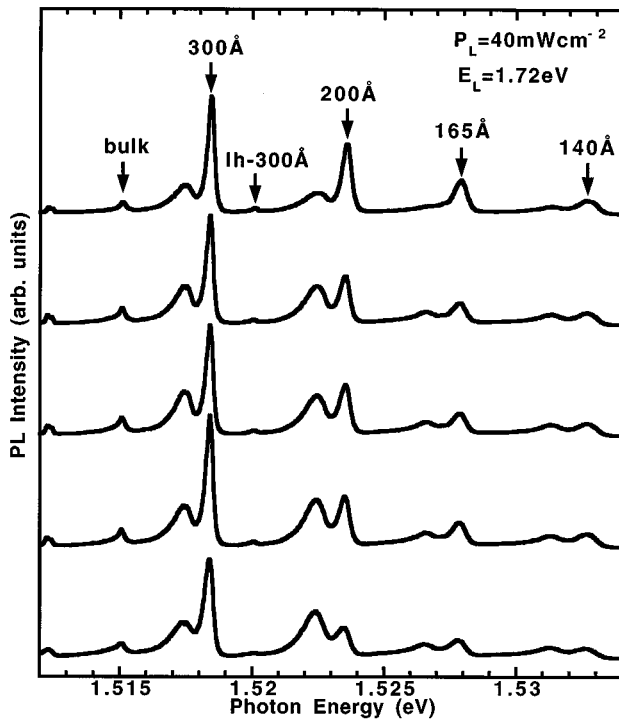


FIG. 6. PL spectra recorded with the laser focused on different regions of sample 1 separated by approximately  $400 \mu\text{m}$ .

can be seen in the lowermost spectrum that the bound exciton transition is more intense than the neutral exciton feature, whereas for the uppermost spectrum the relative intensities of the two transitions is reversed. In contrast, no significant variation in the PL spectrum was observed in PL spectra taken from different regions of samples 2–4.

The PL emitted by the samples was also studied as a function of a magnetic field applied perpendicular to the layers. Spectra were recorded in the Faraday geometry with the incident and emitted light propagating almost parallel to the field axis. Figures 7(a) and 7(b) plot PL spectra, emitted in the  $\sigma^-$  and  $\sigma^+$  circular polarization sense, respectively, of the 300-Å quantum well of sample 1 with different applied fields. Notice the shift of the free-exciton PL peak to higher energy with increasing field ( $B$ ). This shift shows an approximately quadratic dependence with  $B$  at low field, which is characteristic of excitonic transitions. The bound exciton feature also shifts to higher energy with field, but at a rather shallower rate than the free exciton, so that the splitting of the bound and free exciton increases. Notice that around 4 T a third peak emerges just below the free-exciton line in  $\sigma^-$  polarization and forms a well-resolved peak in the 8-T  $\sigma^-$  spectrum, marked  $X_i^+$ . This feature is not observed at 4 T in  $\sigma^+$  polarization, although at 8 T a slight asymmetry appears on the low-energy side of the free-exciton line. Similar behavior was observed for the other quantum wells of sample 2 and the other three samples.

#### IV. ORIGIN OF THE BOUND EXCITON LINE

The temperature dependence of the PL in Fig. 3 demonstrates that the lower-energy component of the doublet emitted from each well is due to a bound exciton. The splitting of

the doublet can be crudely regarded as the binding energy of the exciton to its binding center ( $E_b$ ), yielding values of 0.97–1.35 meV depending on the well width, as listed in Table I. The sharp decline in intensity of the bound exciton peak with temperature, plotted in Fig. 3, agrees well with the dependence  $\exp(-E_b/kT)$ . Physically, the decline in the bound exciton peak with temperature can be understood as due to thermal disassociation of the exciton from its binding center, which occurs when the thermal energy is comparable to the binding energy, i.e., 12–16 K. In this section we discuss the origin of the binding center.

As discussed in the Introduction, previous authors have assigned PL peaks below the energy of the band-edge free exciton to impurity bound excitons or biexcitons. We propose here that rather than an impurity ion, or another exciton, the binding center is in fact a free charge carrier, which is present in the well due to the background impurities in the  $\text{Al}_{0.33}\text{Ga}_{0.67}\text{As}$  barriers. Since MBE-grown  $\text{Al}_x\text{Ga}_{1-x}\text{As}$  is known to be  $p$  type,<sup>19,20</sup> we can expect an excess of holes in the GaAs wells. An excess hole can bind with an exciton to form a positively charged exciton ( $X^+$ ), consisting of two holes and an electron. Hence the low-energy component of the doublet is caused by recombination of an electron-hole pair in  $X^+$  leaving a hole ( $h^+$ ), according to  $X^+ \rightarrow \text{photon} + h^+$ . The binding energy of the hole and neutral exciton of about 1 meV lowers the energy of the  $X^+$  PL relative to  $X$ .

Is the impurity concentration in the barriers sufficient to support a significant population of  $X^+$ ? The measurements of Daniels *et al.*<sup>20</sup> on  $\text{Al}_x\text{Ga}_{1-x}\text{As}$  grown in our MBE chamber yielded a bulk acceptor concentration of around  $5 \times 10^{15} \text{ cm}^{-3}$ , corresponding to an areal density of about  $1.5 \times 10^{10} \text{ cm}^{-2}$  in our 300-Å barriers. Assuming that all the acceptors are ionized, the average separation of two holes in the well will be 800 Å. Since the neutral exciton has a diameter of about 300 Å, the probability of it binding to a hole to form  $X^+$  will indeed be considerable. Indeed we expect  $X^+$  to still be observable for considerably lower barrier acceptor concentrations than that determined by Daniels *et al.* On the other hand, we can expect the impurity concentration in the GaAs wells, and hence the population of impurity bound excitons, to be much lower. Furthermore, the variation in the binding energy caused by the spatial distribution of the impurities in the well will tend to smear the impurity bound PL peak.

The hole density in the wells will be much larger than that of the photoexcited excitons. Notice in Fig. 4 that the lower-energy peak is observed even at the lower excitation intensity of  $0.85 \text{ mW cm}^{-2}$ . Taking the absorption of the 300-Å quantum well at 1.72 eV to be roughly that of bulk GaAs ( $1.7 \times 10^4 \text{ cm}^{-2}$  from Ref. 19 after allowing for the band-gap shift between 295 and 2 K), means that  $\sim 5\%$  of the light incident on the well will be absorbed. Assuming an exciton lifetime of 170 ps (Ref. 21) yields an estimate for the exciton density of  $3 \times 10^4 \text{ cm}^{-2}$ , which corresponds to an average exciton separation of  $\sim 60 \mu\text{m}$  in the quantum well. Even at the highest densities we could study before heating of the sample occurs, the exciton density is only  $8 \times 10^6 \text{ cm}^{-2}$ , which is still several orders of magnitude less than the concentration of holes in the well created by the barrier acceptors. Although localization due to well width fluctuations

may enhance the exciton density in some regions of the well, it seems very unlikely that the biexciton population could be significant compared to that of  $X^+$  at these excitation intensities. In any case, well width fluctuations do not substantially broaden the exciton energy in these samples, as indicated by their very sharp spectral lines.

Our supposition that the bound exciton peak derives from the positively charged exciton was prompted by the striking similarity of these spectra to those recorded on GaAs quantum wells with intentionally doped barriers. Doping the barriers with donors or acceptors produces an excess of either electrons or holes, respectively, in the well. The density of these excess carriers can be varied by either, applying a voltage between a semitransparent Schottky gate and an Ohmic contact<sup>14–17</sup> or by photoexciting electron-hole pairs in the doped barrier layer.<sup>18</sup> At the lowest carrier intensities, a doublet structure is observed in the PL spectra, qualitatively similar to that reported here for nominally undoped quantum wells. For a remotely  $p$ -type-doped 300-Å GaAs quantum well, we measured a doublet splitting of  $(1.0 \pm 0.1)$  meV. This agrees, within experimental error, with the doublet splitting observed here for the 300-Å undoped quantum well of  $(0.97 \pm 0.01)$  meV.

The temperature dependence observed for the lower-energy peak in the doublet is characteristic of the  $X^+$  transition. At 2 K  $X^+$  is stable. However, at the temperatures where the thermal energy  $kT$  approaches the second hole binding energy,  $X^+$  will disassociate into a neutral exciton and a hole,  $X^+ \rightarrow X + h^+$ . For a binding energy of 1 meV this corresponds to a temperature of 12 K. This causes the rapid decline in the intensity of the  $X^+$  transition in the PL spectra of Fig. 3, with a corresponding strengthening of  $X$ . A temperature dependence similar to that in Fig. 3 has been observed for  $X^+$  in  $p$ -type remotely doped quantum wells; see Fig. 2 of Ref. 18.

The magnetic-field dependence shown in Fig. 7 is also qualitatively similar to that observed for both  $p$ -type<sup>18</sup> and  $n$ -type<sup>17</sup> remotely doped quantum wells at low carrier densities. Notice in Fig. 7 that the higher-energy component undergoes a blueshift with field, which is approximately quadratic in  $B$  at low field. This behavior is characteristic of the diamagnetic shift experienced by neutral excitons. The lower-energy component of the doublet also shifts to higher energy with field, but less rapidly than the neutral exciton, so that the doublet splitting increases with field. A very similar increase in the splitting with field was observed for the intentionally remotely doped samples at low carrier density.<sup>17,18</sup> This can be explained<sup>17</sup> by enhancement of the Coulomb interaction between the neutral exciton and the charge carrier, due to the in-plane confinement introduced by the field. Notice in Fig. 7 that a weak peak emerges on the low-energy side of the  $X$  line in  $\sigma^-$  polarization around 4 T and forms a well-resolved peak (marked  $X_t^+$ ) at higher field. This again is characteristic of charged excitonic transitions, since similar behavior has been observed for both  $n$ -type and  $p$ -type remotely doped quantum wells.<sup>17,18</sup> The field-induced peak is due to an excited spin state (spin triplet) of  $X^+$ , for which the spin wave function is symmetric upon interchange of the two holes. The higher-energy spin-triplet transition observed in  $\sigma^+$  polarization<sup>17,18</sup> can just be resolved at 8 T in Fig. 7, as a low-energy shoulder on the neutral exciton peak.

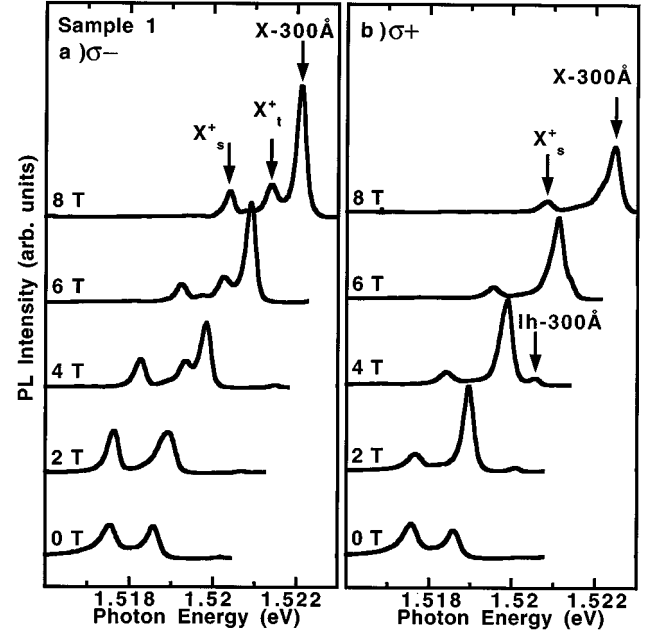


FIG. 7. PL spectra emitted in (a)  $\sigma^-$  and (b)  $\sigma^+$  circular light polarization, on the 300-Å quantum well of sample 1, with different magnetic fields applied perpendicular to the layers.

A detailed description of the spin states of  $X^+$  and  $X^-$  in a magnetic field is presented in Refs. 17 and 18.

Our assignment of the low-energy component in the doublet to  $X^+$  explains the variation in the PL intensities between the four samples studied. As discussed in Sec. II, the  $\text{Al}_{0.33}\text{Ga}_{0.67}\text{As}$  layers of sample 1 are expected to contain a higher background acceptor concentration than those of samples 2–4, producing a larger hole density in the wells. This explains why the  $X^+$  PL peak is more prominent relative to  $X$  for sample 1 than samples 2–4 in Fig. 2. The variation in the PL spectra taken with the light focused on different regions in Fig. 6 indicates that there is also considerable topological variation in the  $\text{Al}_{0.33}\text{Ga}_{0.67}\text{As}$  acceptor concentration in sample 1. Both the difference in the PL doublet of nominally identical samples and the variation of the spectrum across the wafer indicate that the low-energy component cannot be an intrinsic property of the structure. Positively charged excitons due to the background acceptor charge in the barriers provide a plausible extrinsic origin. Clearly, it would be more difficult to explain the variation between samples and across the wafer if the low-energy peak had an intrinsic origin such as biexcitons.

We now consider the well width dependence upon the energy spacing between the two peaks of the doublet in the PL spectra. Table I demonstrates that there is a systematic increase in this splitting with decreasing well width. This can be readily explained by an increase in the second hole binding energy in narrower wells, due to the enhancement in the Coulomb interaction of the hole and neutral exciton.

We have performed a diffusion Monte Carlo method to calculate the second hole binding energies of  $X^+$  as a function of well width. The details of this calculation will be given elsewhere, but it involves essentially a fully three-dimensional calculation in an infinite square-well potential,

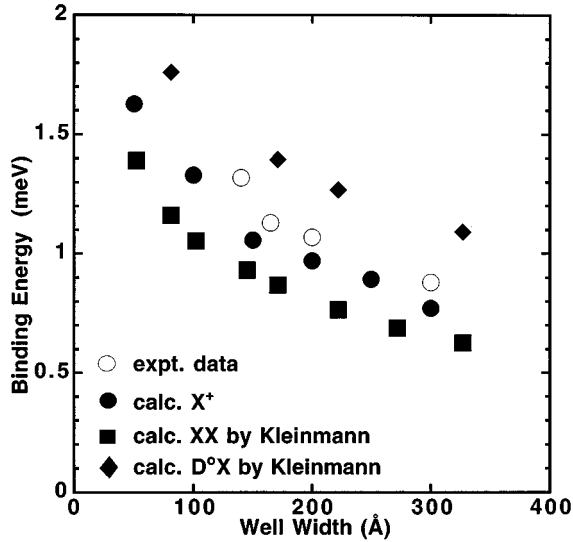


FIG. 8. Well width dependence of the measured doublet splitting (open circles), compared to our calculation of the second hole binding energy in  $X^+$  (solid circles) and the biexciton (solid squares) and donor at center of well (solid diamonds) binding energies calculated by Kleinmann (Ref. 22).

with an effective-mass approximation and mass ratio  $m_e/m_h = 0.3$ . The second hole binding energy is defined as  $E_b = E_{X^+} - (E_X + E_{h^+})$ , where  $E_{X^+}$ ,  $E_X$ , and  $E_{h^+}$  are the energies of an isolated positively charged exciton, neutral exciton, and hole, respectively. The calculated  $X^+$  binding energies plotted in Fig. 8 are in good agreement with the experimental splittings. For comparison we also plot in Fig. 8 Kleinmann's calculation of biexciton binding energies and the binding energies of an exciton to a neutral donor.<sup>22</sup> The biexciton binding energy is found to lie somewhat lower than the experimental data while the energy for binding to a neutral donor turns out to be too large. The best agreement is, in fact, found with the calculated  $X^+$  binding energies, which lends support to this assignment of the experimental data.

We now turn to the illumination intensity dependence of the PL for a laser energy above the barrier band gap (Fig. 5),  $E_L \gg E_{\text{Al}_x\text{Ga}_{1-x}\text{As}}$ , which we explain with reference to Fig. 1, showing the spatial variation of the valence- and conduction-band edges within our structure. The majority of the light incident on the structure will be absorbed in the thick front  $\text{Al}_{0.33}\text{Ga}_{0.67}\text{As}$  layer creating electron-hole pairs. The electric field across the structure, apparent in Fig. 1, spatially separates these photoexcited electron-hole pairs, sweeping the holes into the 140-Å quantum well and the electrons towards the front surface of the structure. This explains the dramatic strengthening of the  $X^+$  peak of the 140-Å quantum well in Fig. 5, since the population of  $X^+$  will increase with the density of holes in the well. Notice that in comparison, the quantum wells lower in the structure show a much less dramatic dependence on the laser intensity in Fig. 5. The modest strengthening of the  $X^+$  peak relative to the  $X$  can be explained by a smaller increase in their hole density due to tunneling from the 140-Å quantum well.

In comparison, a much less pronounced change in the PL line shape with laser power is observed for excitation below

the barrier band gap,  $E_L \ll E_{\text{Al}_x\text{Ga}_{1-x}\text{As}}$ , as can be seen in Fig. 4. The insets to Figs. 4(a) and 4(b) plot the excitation density dependence of the PL intensities of  $X$  and  $X^+$  from the 300-Å well of samples 1 and 2, respectively. We fit the experimental points in the insets with an equation of the form  $I = A(P_L)^\alpha$ , where  $I$  is the intensity of the PL peak and  $A$  and  $\alpha$  are constants. For sample 1, we obtain  $\alpha = 0.98 \pm 0.01$  for the upper-energy peak ( $X$ ), while  $\alpha = 1.22 \pm 0.01$  for lower-energy one ( $X^+$ ). Conversely, for sample 2,  $\alpha = 1.06 \pm 0.01$  for  $X$  and  $\alpha = 1.03 \pm 0.01$  for  $X^+$ . Samples 3 and 4 showed a similar dependence on  $P_L$  to sample 2.

For sample 1, the neutral exciton intensity increases roughly linearly with laser power density ( $P_L$ ), while the positively charged exciton strengthens as  $P_L^{1.25}$ . A qualitatively similar superlinear dependence has been observed by other authors, which led them to conclude that the lower-energy peak is due to the biexciton. However, our measurements on samples 2–4 suggest that this conclusion is unsound. Despite being nominally identical to sample 1, samples 2–4 show only linear strengthening of the low-energy peak with laser power. A similar conflicting dependence on the excitation intensity was found for two samples studied by Charbonneau *et al.*<sup>10</sup> In any case, at the excitation intensities used in our experiments the exciton density is too low for biexcitonic effects, as discussed above.

We believe the variation in the  $X^+$  intensity with laser intensity for  $E_L \ll E_{\text{Al}_x\text{Ga}_{1-x}\text{As}}$  is due to a change in the hole density in the quantum well. As discussed above, the population of electron-hole pairs directly photoexcited in the well is insignificant compared to the hole density produced by the background acceptor concentration of the barriers and can be ignored. A more likely cause of the change in the hole population with light intensity is the photovoltage that will be created by absorption of light in the GaAs buffer layer. We have observed a similar effect in remotely doped quantum wells grown on a thick GaAs buffer layer.<sup>23</sup> This photovoltage will result in holes being swept into the illuminated region of the quantum wells from unilluminated regions. Since the size of the photovoltage will depend on the electric field in the GaAs buffer layer it is quite likely to vary between samples.

## V. BIEXCITONS?

Our conclusion that the low-energy peak in the PL doublet derives from  $X^+$  must cast some doubt over previous assignments of similar structure to biexcitons.<sup>7–10</sup> All these previous experiments were performed on MBE-grown GaAs/ $\text{Al}_x\text{Ga}_{1-x}\text{As}$  quantum wells similar to our own. In Refs. 7–9 PL spectra were recorded with cw illumination intensities comparable to those we used. They observed a doublet structure in the PL spectra with a splitting of between 0.9 and 1.3 meV, very similar to those we report here. Bearing in mind the similarity of the experiments and the observed PL spectra, it seems inconceivable that these authors were observing a different phenomenon from ours.

As discussed above, under the excitation conditions employed by us, as well as the previous workers in Refs. 7–9, the density of exciton is negligible in comparison to that of

the holes created by the barrier acceptors. Under these illumination intensities the biexciton population will be tiny. On the other hand, we have demonstrated that the barrier acceptor concentration will produce a large population of  $X^+$ . The superlinear strengthening of the low-energy peak with laser intensity (for excitation directly in the well) is not necessarily indicative of biexciton formation as argued in Refs. 7–9, since it could be explained by the photoexcitation causing a change in the background hole density in the well.

The line shape of the lower-energy peak, which displays a broader tail on the low-energy side, has been argued to be indicative of biexcitons, since it is produced by the thermal energy distribution of the excitons.<sup>8</sup> Close inspection of the  $X^+$  peaks in Fig. 2 shows that our spectra display this broadening of the low-energy side too. However, this does not mean the peak derives from a biexciton, since the broadening could just as readily be explained by the thermal energy distribution of the holes in the well.

As we pointed out earlier, our measured splittings are somewhat larger than the biexciton binding energies calculated by Kleinmann<sup>22</sup> for GaAs/ $\text{Al}_x\text{Ga}_{1-x}\text{As}$  quantum wells. The values calculated by Kleinmann are plotted in Fig. 8, where it can be seen that although they follow the same trend with well width as that we calculated for  $X^+$ , they lie around 0.15 meV lower in energy. Although the experimental splittings agree best with the binding energy calculated for  $X^+$ , a degree of caution must be exercised in the face of relatively small calculated energy differences. Since the binding energies are sensitive to the parameters and assumptions made in the calculation by an amount up to 0.1 meV or so, it is difficult to make a definite distinction on the basis of the calculations alone.

Confirmation that the low-energy peak is caused by the presence of holes, rather than excitons, in the well, comes from the laser power dependence for excitation of the front barrier region. In this case we see a dramatic strengthening of the low-energy peak of the upper well due to photoexcited holes being swept into the well. This behavior would be difficult to explain with the biexciton assignment.

Finally, we comment briefly upon the large number of exciton dephasing studies in GaAs quantum wells that have also been interpreted as providing evidence for the existence of biexcitons.<sup>8,9,24</sup> In particular, the observation of a degenerate four-wave mixing (DFWM) signal at negative time delays suggests the presence of exciton-exciton interactions.<sup>24</sup> It should be borne in mind, however, that these pulsed-laser experiments typically generate much larger exciton densities than cw PL measurements such as ours. For instance, strong exciton-biexciton quantum beat phenomena were reported in Ref. 4 for laser powers estimated to correspond to exciton densities of  $\sim 3 \times 10^{10} \text{ cm}^{-2}$ , which is comparable to the background hole density that we estimated above for our samples. This contrasts with the situation under cw illumination, as in our experiments, where the exciton density will be several orders of magnitude smaller. Clearly then, the contribution of biexcitons to the DFWM signal cannot be ignored, as it can be for typical cw PL experiments. On the other hand, the effect of the sizable background hole concentration (due to the barrier acceptors) also cannot be ignored in the interpretation of the DFWM experiments and could perhaps provide an explanation for the sample-dependent

anomalies noted in the polarization dependence of the DFWM signal.<sup>24</sup> A description of DFWM that includes positively and negatively charged excitons, originating from photoexcited, as well as background, charge in the well remains a theoretical challenge.

## VI. CONCLUSION

The PL spectra of high-quality MBE-grown GaAs/ $\text{Al}_{0.33}\text{Ga}_{0.67}\text{As}$  quantum wells display a doublet structure at temperatures below about 10 K. A systematic study of the spectra has shown that the upper and lower components of this doublet derive from the band-edge neutral and positively charged excitons, respectively.  $X^+$  is formed due to the presence of holes in the well produced by ionization of acceptors in the barrier layers. These acceptors were not intentionally introduced to the  $\text{Al}_{0.33}\text{Ga}_{0.67}\text{As}$ , but unavoidably incorporate during MBE growth. This extrinsic origin for the lower-energy peak of the PL doublet provides an explanation for the difference in spectra taken on samples grown at different times and the variation in the PL line shape measured across the surface of one of the wafers.

Our assignment of the low-energy peak in the doublet to  $X^+$  was motivated by the striking similarity of the PL spectra to those taken on samples with acceptors deliberately introduced to the barriers. The energy splitting of the doublet observed in the remotely doped samples is the same as that observed for nominally undoped quantum wells of the same width. Furthermore, the PL spectra of the samples with undoped and doped barriers show a qualitatively similar evolution with temperature and magnetic field. The low-energy peak weakens sharply with increasing temperature due to the thermal dissociation  $X^+ \rightarrow X + h^+$ . Under a magnetic field applied normal to the wells there is a large increase in the doublet splitting, due to the increase in the second hole binding energy of  $X^+$  caused by the magnetic confinement. We also observe the emergence of a new peak in the PL emitted in  $\sigma^-$  circular polarization under an applied field, due to the excited spin-triplet state of  $X^+$ . Both the field-induced transition and the increase in the doublet splitting is characteristic of the  $X^+$  transition.

The second hole binding energy of  $X^+$  also increases with the enhanced confinement produced by a narrower quantum well. This explains the observed increase in the doublet splitting of  $X$  and  $X^+$  with decreasing well width. A Monte Carlo calculation of the second hole binding in  $X^+$  (Fig. 8) is in good agreement with the observed doublet splitting over the range of well widths studied.

Our assignment of the  $X^+$  peak is confirmed by its strengthening with the hole density in the well. When the sample is illuminated with laser light of energy higher than the barrier band gap, the internal electric field separates electron-hole pairs photoexcited in the front thick  $\text{Al}_x\text{Ga}_{1-x}\text{As}$  region, sweeping holes into the upper quantum well. This produces a sharp strengthening of the  $X^+$  PL peak of the upper quantum well. A less dramatic strengthening of the  $X^+$  peak of the lower wells arises from tunneling of holes deeper into the structure.

Since the intensity of the  $X^+$  peak is sensitive to areal hole densities of  $10^{10} \text{ cm}^{-2}$  or less, low-temperature PL spectroscopy could provide a very sensitive tool for studying

the acceptor concentration of the  $\text{Al}_x\text{Ga}_{1-x}\text{As}$  barriers. Indeed, we observed significant differences in the  $X^+$  intensity measured on samples grown at different times and across the surface of one of the samples. The background barrier acceptor concentration is of interest because it limits the performance of several quantum well devices. For instance, the barrier acceptor charge is also known to degrade the performance of  $p$ - $i$ - $n$  multiple quantum-well optical modulators since it causes a field drop between successive wells within the (nominally) intrinsic region. This technique of studying

the low-temperature  $X^+$  PL intensity could also be useful for characterization of devices grown by other methods, such as metal-organic chemical-vapor deposition or metal organic vapor phase epitaxy where the  $\text{Al}_x\text{Ga}_{1-x}\text{As}$  acceptor contamination is usually greater than for MBE.<sup>19</sup>

#### ACKNOWLEDGMENT

Part of this research (at Cavendish Laboratory) was funded by EPSRC, UK.

\*Also at Cavendish Laboratory, Madingley Road, Cambridge CB3 0HE, United Kingdom.

<sup>1</sup>See, for instance, H. Künzel and K. Ploog, in *Gallium Arsenide and Related Compounds*, IOP Conf. Proc. No. 56 (Institute of Physics and Physical Society, London, 1981), Chap. 8.

<sup>2</sup>J. J. Hopfield, Phys. Rev. **112**, 1555 (1958).

<sup>3</sup>D. S. Citrin, Phys. Rev. B **47**, 3832 (1993); L. C. Andreani, F. Tassone, and F. Bassani, Solid State Commun. **77**, 641 (1991).

<sup>4</sup>D. C. Reynolds, K. K. Bajaj, C. W. Litton, P. W. Yu, W. T. Masselink, R. Fischer, and H. Markoc, Phys. Rev. B **29**, 7038 (1984).

<sup>5</sup>B. V. Shanabrook and J. Comas, Surf. Sci. **142**, 504 (1984); D. C. Reynolds, C. E. Leak, K. K. Bajaj, C. E. Stutz, R. L. Jones, K. R. Evans, P. W. Yuand, and W. M. Theis, Phys. Rev. B **40**, 6210 (1989); X. Liu, A. Petrov, B. D. McCombe, J. Ralston, and G. Wickes, *ibid.* **38**, 8522 (1988).

<sup>6</sup>R. C. Miller, A. C. Gossard, W. T. Tsang, and O. Munteanu, Solid State Commun. **43**, 519 (1982); P.O. Holtz, M. Sundaram, J. L. Merz, and A. C. Gossard, Phys. Rev. B **40**, 10 021 (1989).

<sup>7</sup>R. C. Miller, D. A. Kleinman, A. C. Gossard, and O. Munteanu, Phys. Rev. B **25**, 6545 (1982).

<sup>8</sup>R. T. Phillips, D. J. Lovering, G. J. Denton, and G. W. Smith, Phys. Rev. B **45**, 4308 (1992); Phys. Rev. Lett. **68**, 1880 (1992).

<sup>9</sup>G. O. Smith, E. J. Mayer, J. Kuhl, and K. Ploog, Solid State Commun. **92**, 325 (1994).

<sup>10</sup>S. Charbonneau, T. Steiner, M. L. W. Thewalt, Emil S. Koteles, J. Y. Chi, and B. Elman, Phys. Rev. B **38**, 3583 (1988).

<sup>11</sup>Although we refer to charged excitons and biexcitons as *bound* excitons, it should be noted that in principle they are able to move in the quantum-well plane. They are *bound* in the sense that the center-of-mass motion of the neutral exciton is subject to additional binding.

<sup>12</sup>K. Kheng, R. T. Cox, Y. M. d'Aubique, F. Bassim, K. Saminadayar, and S. Tatarenko, Phys. Rev. Lett. **71**, 1752 (1993).

<sup>13</sup>K. Kheng, R. T. Cox, M. Mamor, K. Saminadayar, and S. Tatarenko, J. Phys. (France) IV **3**, C5-95 (1993).

<sup>14</sup>A. J. Shields, C. L. Foden, M. Pepper, D. A. Ritchie, M. Grimshaw, and G. A. C. Jones, Superlatt. Microstruct. **15**, 355 (1994).

<sup>15</sup>A. J. Shields, M. Pepper, D. A. Ritchie, M. Y. Simmons, and G. A. C. Jones, Phys. Rev. B **51**, 18 049 (1995).

<sup>16</sup>G. Finkelstein, H. Shtrikman, and I. Bar-Joseph, Phys. Rev. Lett. **74**, 976 (1995).

<sup>17</sup>A. J. Shields, M. Pepper, M. Y. Simmons, and D. A. Ritchie, Phys. Rev. B **52**, 7841 (1995).

<sup>18</sup>A. J. Shields, J. L. Osborne, M. Y. Simmons, M. Pepper, and D. A. Ritchie, Phys. Rev. B **52**, R5523 (1995).

<sup>19</sup>*Properties of Aluminium Gallium Arsenide*, edited by S. Adachi (INSPEC, London, 1993), p. 289.

<sup>20</sup>M. E. Daniels, P. J. Bishop, K. O. Jenson, B. K. Ridley, D. A. Ritchie, M. Grinshaw, E. H. Linfield, G. A. C. Jones, and G. W. Smith, J. Appl. Phys. **74**, 5606 (1993).

<sup>21</sup>This value was reported for a high-quality 270-Å GaAs QW at low exciton density by R. Eccleston, B. F. Feuerbacher, J. Kuhl, W. W. Rühle, and K. Ploog, Phys. Rev. B **45**, 11 403 (1992).

<sup>22</sup>D. A. Kleinmann, Phys. Rev. B **28**, 871 (1983).

<sup>23</sup>A. J. Shields, J. L. Osborne, M. Y. Simmons, D. A. Ritchie, and M. Pepper, Semicond. Sci. Technol. (to be published).

<sup>24</sup>J. Kuhl, E. J. Mayer, G. Smith, R. Eccleston, D. Bennhardt, P. Thomas, K. Bott, and O. Heller, in *Coherent Optical Interactions in Semiconductors*, Vol. 330 of *NATO Advanced Study Institute, Series B: Physics*, edited by R. T. Phillips (Plenum, New York, 1994), p. 1, and references therein.